

Characterization of Activated Carbon Nano-materials prepared from Sugarcane Bagasse and its Effectiveness for Removal of Arsenic from Aqueous Solution

Arti Gupta¹, Vinod Kumar², Prerna Rathaur³, Richa Singh⁵, Abhishek Madhesiya⁵ and Pramod Kumar Singh^{6*}

^{1,2,3,4,6*}Babu Banarasi Das University (School of Basic Science, Department of Environment Science), Lucknow, (Uttar Pradesh), INDIA

⁵Babu Banarasi Das Institute of Technology and Management (Department of Physics), Lucknow, (Uttar Pradesh), INDIA

ORCID id: 0000-0003-0061-6609

Abstract: The purpose of the current study is to characterize activated nano-carbon developed from sugarcane bagasse (ACSB) through physical activation and evaluate effectiveness it in removing arsenic from contaminated water. Sugarcane bagasse was used due to cellulose-containing, fibrous in nature, readily available, and inexpensive raw materials. Elemental analysis revealed that the activated carbon comprised 88.93% carbon, 9.75% oxygen, 0.75% silicon, and 0.56% chloride by mass. Morphological analysis indicated a honeycomb-like surface structure with clean, well-defined pores. Textural characterization showed a pore volume of 0.0252 cc/g, a pore width of 1.6137 nm, and an average pore diameter of 3.688 nm. The micropore volume and area were 1.325×10^{-3} cc/g and $18.11 \text{ m}^2/\text{g}$, respectively. The Dollimore-Heal (DH) method determined the adsorption and desorption surface areas to be $30.76 \text{ m}^2/\text{g}$ and $47.17 \text{ m}^2/\text{g}$, with corresponding pore volumes of 3.022×10^{-3} cc/g and 1.907×10^{-3} cc/g. Arsenic-contaminated water (30 ppb) was treated with ACSB under varying conditions of dosage, pH, contact time, and agitation speed. Optimal removal efficiency was achieved with 2.0 g/100 mL dosage (88% removal), pH 8 (86% removal), 60 rpm agitation speed (88.5% removal), and 90 minutes contact time (88.47% removal). These findings demonstrate that ACSB is a promising, cost-effective adsorbent for arsenic remediation, transforming agricultural waste into an efficient solution for water purification.

Keywords: Adsorption, Desorption, Removal, Arsenic, Nanocarbon tube

1. INTRODUCTION

Humans are well aware of the toxicity of the arsenic [1]. Human health is at risk from long-term exposure of arsenic in drinking water [2]. Long-term exposure to water contaminated with arsenic has been linked to negative consequences on people's neurological systems, digestive tracts, skin, and lungs [1], [3]. Due to both natural geological processes and human activities including mining, metallurgy, and the chemical industry, arsenic is widely distributed in natural water [4], [5].

The problem of water pollution caused by arsenic contamination is worldwide for long time, with reports indicating that over 100 million people worldwide have been adversely affected by drinking arsenic contaminated water [6]. The elimination of arsenic from water has been a pressing issue, and lowering the level of arsenic in drinking water will have a positive impact on people's health. As a result, in recent decades, the relevant standards have had stricter arsenic contamination acceptability thresholds for drinking water [7]. The World Health Organization (2011) updated its regulation to lower the maximum allowable level of 10 $\mu\text{g}/\text{L}$ for arsenic concentration in drinking water from 50 $\mu\text{g}/\text{L}$ [8] [9]. In natural water, arsenic typically exists in two valence states: As(III) and As(V). In neutral conditions, As(III) primarily exists as a molecular form, whereas As(V) primarily exists as H_2AsO_4 or HAsO_4^{2-} . As a result, As(III) can be converted into As(V) by chemical or biological methods to reduce its toxicity and the difficulty of subsequent treatment [10], [11] & [12].

The three primary techniques for removing As(V) from drinking water are membrane technology [13], [14], coagulation technology [15], [16], and adsorption technology [17], [18], [19]. Adsorption technology has been widely utilized to clean arsenic-contaminated water because of its many benefits, including easy operation, financial gains, and a wide range of materials which may act as adsorbents. However, the cost of production and regeneration of commercial activated carbons remains high. Activated carbon was used extensively in the sorption of heavy metals from contaminated wastewater due to it's a versatile adsorbent with optimal sorption qualities. It is commonly recognized that activated carbon, a type of carbide produced by carbonization and activation procedures from coconut shell, charcoal, lignin, sawdust, rice husk, and other carbonaceous materials. The large specific surface area, surface functional groups, and rich pore structure are responsible for the significant adsorption ability [17]. Prepared activated carbon from *Typha* leaf and reported up to 99% removal of As (V) at 1.5 g/100 ml solution [20].

Agricultural waste are valuable sources of inexpensive raw materials for natural bio-adsorbents because of their richness and accessibility. It takes a significant amount of carbon content to convert biomass into activated carbon. The chemical composition of sugarcane bagasse is composed of 25% hemicellulose, 50% cellulose, and 25% lignin, with a total carbon content of 24.7% [21] [22]. Activated carbon has a micro-porous structure due to its high cellulose content [23] [24]. Therefore, activated carbon can be produced using sugarcane bagasse [25]. The activation of rice husk results in a highly porous carbon with a large surface area [21]. According [26] to the maximum efficiency for removal of Cr ⁶⁺ was 99.78% at <1.0 pH by chemical method. A growing body of research is being done on the manufacture of activated carbon from agricultural waste materials, which can be used to create value-added products with a variety of environmental uses [24].

The present studies aims to explore low cost production of adsorbent which may easily available like sugarcane bagasse an agricultural biowaste. So, the sugarcane bagasse was used to prepare activated carbon through physical and chemical activation and characterized them. The different parameters such as the optimization of the effect of dose, pH, contact time and agitation speed were studied.

2. Materials and Methods

Materials

All chemicals used were of AR grade. The glassware and sample bottles which used for the study washed with 10% HNO₃ followed by rinsed with distilled water 3-4 times. Standard Arsenate Solution (1000 mg/L) CRM was supplied from MERCK Company which used to make different working solution for calibration and known stock of 30 ppb. Double distilled water was used to prepare all aqueous solution.

Preparation of activated carbon from Sugarcane Bagasse (ACSB)

Sugarcane bagasse (SB) which is easily available was used for preparation of activated carbon. SB was collected from local sugarcane vendors. SB was cut manually into average sizes approx. 3 cm and washed thoroughly with tap water to remove dirt and impurities. To achieve more purity and for decontamination purposes, bagasse was further washed with deionized water. In order to dry it completely, sugarcane bagasse was left out in the sun for few days. Then it further dried in oven 105 °C to remove moisture content. These dried plant materials were packed in a sealed container for experimentation. ACSB was prepared in absence of oxygen. Sealed plant materials carbonized by adjusting the furnace temperature at desired activation temperature (550°C) for 01 hr. After carbonization, the ACSB was washed with distilled water 3-4 times than 0.1 M HCl to remove ash content then it again washed with distilled water. The ACSB was dried at 105 °C for four hours in an oven. After being dried, the sample was passed through a 100-mesh filter and stored in desiccators until used again.

Morphological characterization of ACSB:

Energy-dispersive X-ray (EDX)

An EDX technique was used for the assessment of elemental composition of ACSB. At 20.00 kV, Energy-dispersive X-ray (EDX) 6510, LA, was utilized to characterize the elemental composition of ACSB.

Scanning Electron Microscope (SEM)

SEM was used to create a high resolution image by scanning an object's surface, produces detailed, magnified images of the object. SEM images was obtained with a field emission scanning electron microscope (Carl Zeiss NTS GmbH, Oberkochen (Germany) Model: SUPRA 40 V P operated at an accelerating voltage of 10 kV.

X-ray diffraction Technique

To assess the material's chemical composition, physical properties, and crystallographic structure, a nondestructive method was used as XRD. Hecus X-Ray Systems GmbH, Graz (Austria) Model: S3 MICRO was used to record the X-ray diffraction (XRD) patterns of activated carbon at room temperature. In order to analyze the samples for activated carbon, they were exposed to monochromatized Cu K α radiation (1.5406 Å) at temperatures ranging from 5 to 80°C. The 45 kV operating voltage and 40 mA operating current were utilized, respectively. With a sweep of 5° min $^{-1}$, the time constant of 3.0 s was maintained. A focused X-ray beam interacts with a sample in a way that causes some of the beam to be transmitted, some to be absorbed by the sample, some to be diffracted, dispersed, and refracted. By using Bragg's Law, these diffracted beams can be measured.

$$n\lambda = 2d\sin\theta$$

Where n is number of diffraction pattern (n=1 for first order, n=2 for second order=3 for third order), d is the distance between adjacent atomic planes, θ is the angle of incidence of the X-ray beam, and λ is the wavelength of the incident X-ray beam. The Debye–Scherrer equation was used to determine average particle sizes. The peaks in the prepared sample were interpreted using JCPDS.

Brunauer-Emmett-Teller (BET)

BET technique was used to assess the surface area, pore volume and pore diameter of the materials which is based on adsorption of gas on a surface the materials. The surface area can be calculated from the amount of gas adsorbed at a given pressure. Quanta chrome Autosorb 1C was used to analyze the surface area and the pore size of ACSB. Nitrogen adsorption–desorption isotherms were used to determine the pore volumes and adsorption/desorption isotherms of the adsorbents. Before starting the N₂ adsorption process, the samples were vacuum-stored at 200°C. The Brunauer–Emmet–Teller (BET) equation and the single point approach were utilized ascertain the total surface area and pore volume, respectively. The t-plot approach was used to determine microporosity. Using the Barret–Joyner–Halenda (BJH) method, the pore size distribution in the adsorption isotherm was determined. H₂ gas was used in chemisorption to assess the active metal surface area. Each sample weighed 0.1 g before it was placed into a capillary glass tube. The samples were then degassed for six hours at 25 °C in a nitrogen

environment. The nitrogen adsorption and desorption spectra were measured at 77K by using a Quanta-chrome Autosorb-1 BET analyzer.

Adsorption Studies

A thorough description of the two-stage equilibrium was necessary for the effective modeling of the dynamic separation of the adsorption of a solution by an adsorbent. When the amount of dissolved material on the adsorbent equals the amount of adsorption, adsorption equilibrium was reached. The two most popular models for explaining experimental adsorption data were used as Langmuir isotherm and Freundlich isotherm in the present studies.

Langmuir Isotherm

The Langmuir equation was obtained from a basic mass-action kinetic. This model was predicated on the ideas that once a molecule occupies a site, no more sorption occurs and that the forces of contact between adsorbed molecules were insignificant. Once the saturation point was reached, no more sorption occurs. The equation for the Langmuir isotherm can be expressed as:

$$\frac{C_e}{q_e} = \frac{1}{Kq_{max}} + \frac{C_e}{q_{max}}$$

where K and q_{max} are the Langmuir constants associated with the adsorption capacity and intensity; C_e is the equilibrium concentration of the adsorbate solution; and q_e is the quantity of adsorbate adsorbed per gram.

Freundlich isotherm model

The multi-layer adsorption on the adsorbent surface was allowed by the above isotherm model. The Freundlich isotherm equation can be written as follows:

$$\ln q_e = \ln k_f + \frac{1}{n} \ln C_e$$

q_e was the amount of adsorbate adsorbed per g; n is the energy of intensity or adsorption; k_f is the Freundlich constant associated with adsorption capacity; and C_e is the adsorbate solution's equilibrium concentration.

Batch Adsorption Experiment

Atomic absorption spectrophotometer (Perkin Elmer Analyst 300) was used for the determination of arsenic concentration in the solution after removal. To assess the arsenic removal efficiency by ACSB from contaminated water, a known solution of arsenic (30 $\mu\text{g L}^{-1}$) was prepared by using an arsenate stock solution of 1000 mg L^{-1} (As_2O_5) in glass distilled water. Through batch model, the adsorbent dose, pH, contact time, and agitation speed were adjusted as per Table-1, to improve the adsorption of arsenic ions onto the adsorbent. Different doses of activated carbon i.e., 0.5, 1.0, 1.5, 2.0, and 2.5 g/100 ml were used in the known solution of arsenic (30 $\mu\text{g L}^{-1}$) and shaken at constant speed at 60 rpm for 180 minutes. The equilibrium data were obtained by As (V) onto prepared ACSB. Then, the performance of the best dose of AC was selected based on the maximum

removal percentage. A control sample was taken before getting in contact with the activated carbon to determine the exact concentration of adsorbate. The filtrates were used to analyze arsenic concentration by AAS after filtration using Whatman no. 42 filter paper.

Table 1. Different variables were used in batch adsorption experiment

Parameters	Variables	Constant
Effect of Adsorbent	Adsorbent Dose (range 0.5 to 2.5 g)	pH, Contact Time, Agitation Speed
Effect of pH	pH (range 2.0 to 10.0)	Adsorbent Dose, Contact Time Agitation Speed
Effect of Contact Time	Time (range 60 to 180 min.)	Adsorbent Dose, pH, Agitation Speed
Effect of Agitation Speed	Agitation Speed (range 40 to 120 rpm)	Adsorbent Dose, pH, Contact Time

Determination of arsenic concentration

The final concentration of Arsenate (As [V]) was determined using AAS. The percentage removal and the amount of Arsenate adsorbed onto AC were calculated according to the following equations:

$$\text{Arsenic } (\mu\text{g/g}) = \frac{\text{Initial As concentration } (\mu\text{g/L}) - \text{Concentration of As at equilibrium}}{\text{Mass } (g)} \times \text{Volume}$$

$$\% \text{ removal} = \frac{\text{Initial As concentration } (\mu\text{g/L}) - \text{Concentration of As at equilibrium}}{\text{Initial As concentration } (\mu\text{g/L})} \times 100$$

Statistical Analysis

The results were analyzed using Sigma stat 4 software. As a comparative analysis, the unpaired 't'-test was performed. The probability value was found less than 0.05 ($P < 0.0001$) and was considered statistically significant.

3. Results and Discussion

Characterization of ACSB

Scanning electron microscopy (SEM) was used to assess the surface morphology and physical appearance of the ACBS (Fig 1 a, 1b and 1c). Pores of various sizes and shapes were visible in the SEM. A well-developed porous surface was seen in activated carbons at increased magnification. SEM indicated that clear appearance of honey comb like structure (Fig.1c) as well as carbon nano-tube appeared at 1000 magnification (Fig.1b) and micro-pores clearly appeared at magnification on 1280x960 pixel (Fig.1d). Appearance of these structures in ACSB increased the surface area of the materials which was clear by BET.

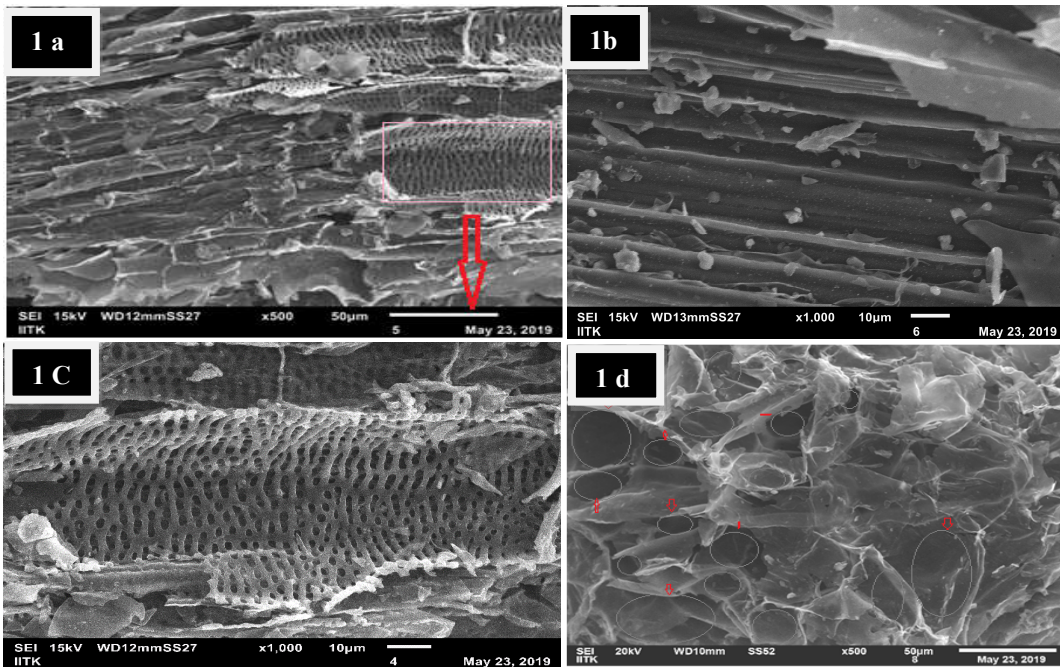


Fig. 1: Scanning Electron Microscopy of activated carbon prepared from sugarcane bagasse showing surface morphology at different magnification (a) at 500 magnification (1b) Carbon nanotube at 1000 magnification (1c) Honey comb like structure at 1000 magnification (1d) Micro-pores clearly appeared at magnification on 1280x960 pixel.

Activated carbon generated from sugarcane bagasse was found to have 88.93% carbon by mass as per observation of EDX, with additional components such as oxygen (9.75%), silicon (0.75%), and chloride (0.56%) also present (Table 3 and Fig. 2d). The characteristic properties of ACBS was studied with XRD, carried out by Rigaku Ultima-IV X-ray diffractometer shown in (Fig. 2a). The XRD pattern showed broad diffuse scattering at 10°-28°, which confirmed the short range order characteristic of the amorphous nature of ACSB and few crystalline peaks were also observed. It may be due to presence of silicon in the materials (Fig. 2a). Based on BET results, a graph was plotted between the volume of nitrogen gas and its relative pressure (Fig. 2b).

Texture of ACBS indicated that total pore volume was 2.315×10^{-2} cc/g with average pore diameter 3.688 nm while the pore volume was 0.025.2 cc/g with pore width 1.6137 nm. The micro-pore area was $18.11 \text{ m}^2/\text{g}$ and micro-pore volume was 1.325×10^{-3} cc/g (Table 2). In order to characterize the surface morphology of adsorbents, SEM was conducted to characterize the activated carbon by different workers [27], [20]. Langmuir surface area was $4.292 \times 10^2 \text{ m}^2/\text{g}$. Different method were used to assessed the adsorption and desorption surface area. Dollimore and Heal (DH) cumulative adsorption surface area was 30.76 m^2/g while desorption surface area was 47.17 m^2/g and DH method adsorption and desorption pore volume were 3.022×10^{-3} cc/g and 1.907×10^{-3} cc/g respectively while BJH method adsorption and desorption surface area were $29.76 \text{ m}^2/\text{g}$ and 47.17 m^2/g respectively (Table 2). The volume of micropore was substantially greater than that of the mesoporous, indicating that the micropore was involved in the kinetics of adsorption. Thus, the activated carbon prepared from sugarcane bagasse (ACSB) may be act as good adsorbent due to its high adsorption capacity, high surface area, micropore structure and a high degree of surface which was agreement with other worker [28]. The chemical composition and pore structure of ACSB typically determined the sorption activity of the materials.

Table 2. Characterization of activated carbon prepared from sugarcane bagasse (ACBS).

Morphological Properties		Activated Carbon
<i>Pore size and pore volume</i>		
Total Pore Volume(cc/g)		2.315x10 ⁻²
Average Pore Diameter (nm)		3.688
Micro-pore volume (cc/g)		1.325 x10 ⁻²
Micro pore area(m ² /g)		18.11
Pore volume (cc/g)		0.0252
Pore width (nm)		1.6137
<i>Langmuir surface area (m²/g)</i>		
DH Method Cumulative Adsorption surface area (m ² /g)		30.76
DH Method Desorption surface area (m ² /g)		47.17
BJH Method Cumulative Adsorption surface area (m ² /g)		29.76
BJH Method Desorption surface area (m ² /g)		41.23
t- Method External surface area (m ² /g)		7.001
t- Method micro pore surface area (m ² /g)		18.11
DR Method Cumulative Surface Area (m ² /g)		52.85
DH Method Adsorption pore volume (cc/g)		3.022 x 10 ⁻³
DH Method Desorption pore volume(cc/g)		1.907 x 10 ⁻³

Table 3: Elemental composition of activated carbon prepared from sugarcane bagasse (ACSB).

Chemical formula	Mass (%)	Atom (%)	Sigma	Net	K ratio	Line
Carbon (C)	88.93	91.90	0.05	110396	0.0626264	K
Oxygen (O)	9.75	7.56	0.11	3811	0.0073424	K
Silicon (Si)	0.76	0.34	0.02	5091	0.0035234	K
Chloride (Cl)	0.56	0.19	0.02	3268	0.0029871	K
Total	100	100				

The kinetics of materials is indicated in Fig.2c which followed pseudo first order kinetics ($R = -0.94117$). Langmuir Isotherm and Freundlich isotherm were also drawn which indicated in Fig.3a and 3b respectively. ACSB followed Freundlich isotherm having $R=0.89259$ than the Langmuir isotherm ($R=0.77125$). Thus, ACSB act as multilayered adsorbent with different carbon nano tube and honey comb like structure. The kinetics of materials was indicated in Fig.2c which followed pseudo first order kinetics ($R = -$

0.94117). Langmuir Isotherm and Freundlich isotherm were also drawn which indicated in Fig.3a and 3b respectively. ACSB followed Freundlich isotherm having $R=0.89259$ than the Langmuir isotherm ($R=0.77125$). Thus, ACSB act as multilayered adsorbent with different carbon nano tube and honey comb like structure.

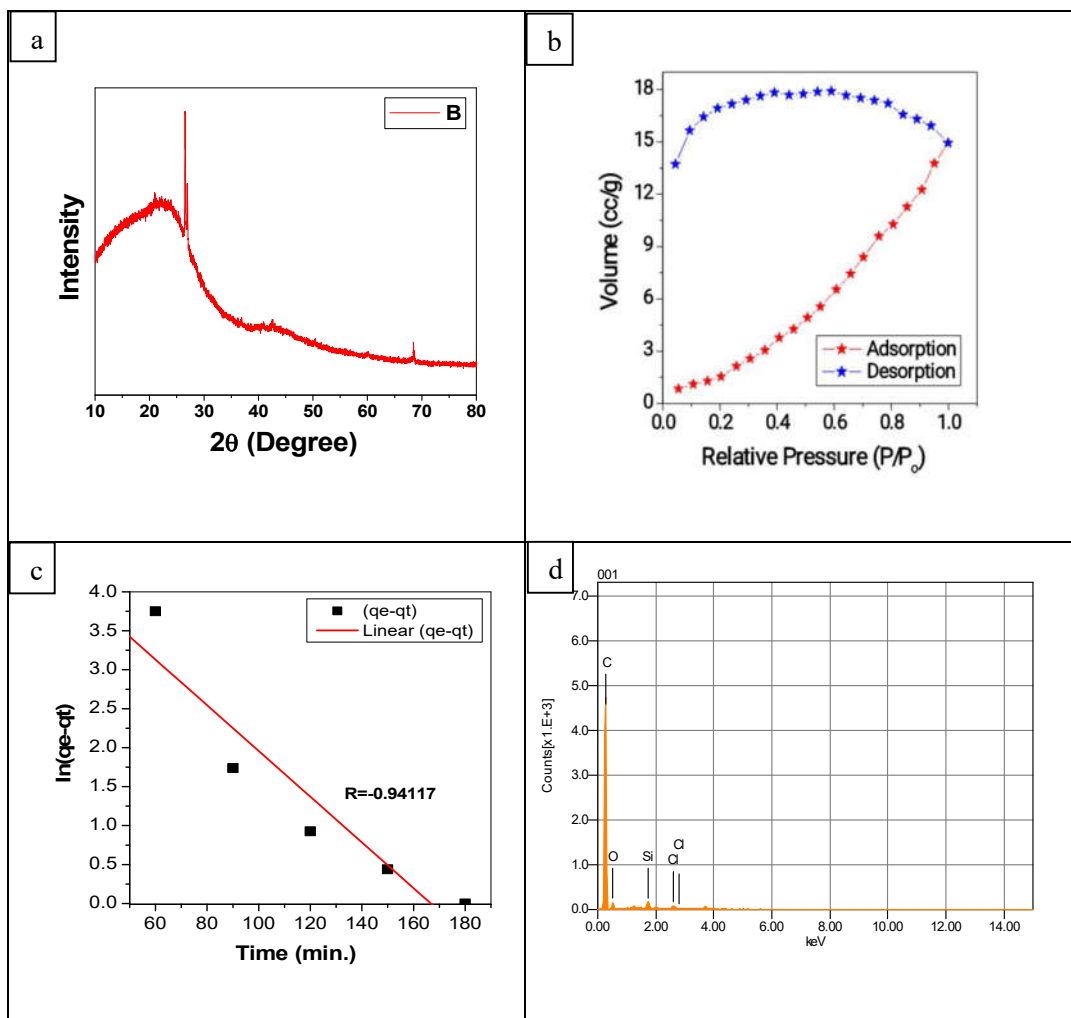


Fig. 2: Characterization of activated carbon prepared from sugarcane bagasse (a) XRD of AC indicating amorphous nature (b) BET based relative graph between volume of N2 gas and pressure to assess the adsorption and Desorption (c) Pseudo-first order kinetics (d) EDX showed elemental composition of AC.

Batch experiment for removal of Arsenic from waste water

The arsenic removal efficiency of activated carbon prepared from sugarcane bagasse (ACSB) was assessed in batch experiment at different condition including adsorbent dose, pH, time and agitation speed to get maximum removal capacity.

Effect of pH

The pH range used in these investigations was 2 to 10. As the pH increased to 8 (86% removal), the removal of As (V) ions increased and then continued to fall (Fig. 4b). Thus, a pH of 8 was found to be optimal for removal. According to [29], at these pH values, As (V) ions were moved to the surface of ACSB, followed by desorption, and the formation of a surface complex. One of the most crucial factors influencing the adsorption process is pH. The degree of ionization, speciation of the surface functional groups, and the surface charge of the adsorbent are all influenced by the pH of the solution [30].

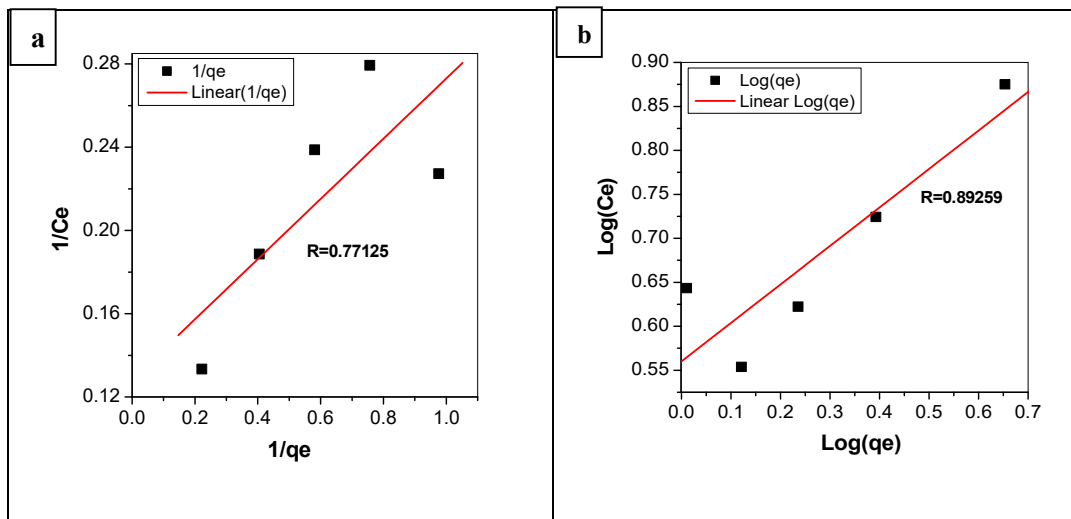


Fig. 3 : The ACSB showed (a) Langmuir Isotherm and (b) Frendlich Isotherm.

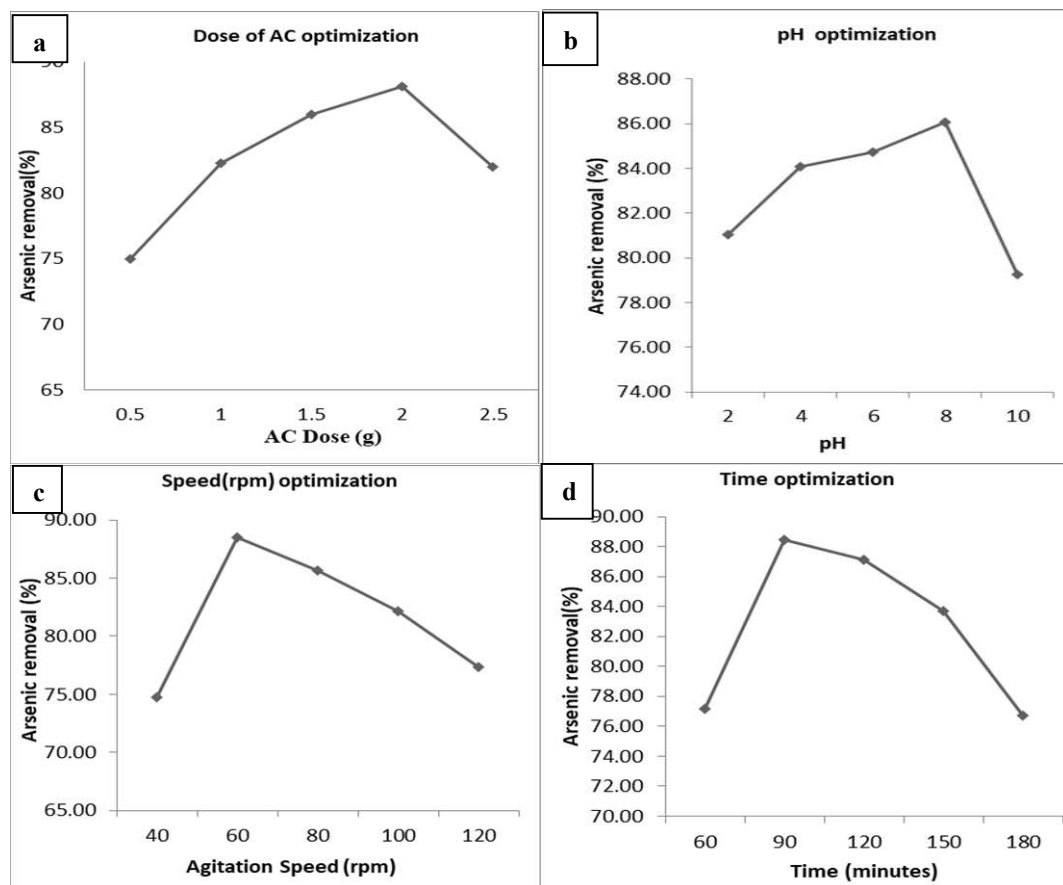


Fig.4: Adsorption optimization of Arsenic from waste water by activated carbon prepared by bagasse an agricultural waste of sugarcane at different condition i.e. (a) Doses of AC optimization (b) pH optimization, (c) Agitation speed optimization and (d) Time optimization.

Effect of dose

Adsorbent doses play a crucial role in adsorption investigations as they establish the adsorbent's capacity for a certain starting As (V) ion solution concentration. According to

Figure 4a, the percentage of removal of As(V) rose to 2 g/100 ml (88.1% removal) at first, but then drastically fell as the adsorbent dose was increased. This might have happened as a result of the higher dose of adsorbents making more exchangeable sites accessible for the ions in the solution. As adsorbent dosage was increased, the result shown in **Fig. 4a** indicated that 2.0g was the ideal dose for removing As (V) ions from aqueous solution. The removal efficiency decreased with increasing adsorbent dose beyond the optimal level. [31] found a similar result when using activated carbon made from Typha to remove Cd(II). They claimed that the rise in adsorption site un-saturation brought on by the adsorption reaction is the primary cause of the decrease in adsorption capacity with increasing adsorbent dose. Particle interactions brought on by high sorbent concentration, like aggregation, could be another cause. The sorbent's overall active surface area would diminish as a result of this aggregation.

Effect of time on As (V) ion adsorption

One of the crucial parameters is the impact of the contact time between the adsorbent particles and the adsorbate. The contact period was altered from 60 to 180 minutes in the current study. The when(V) ion was removed with a fast increase at first, reaching an 86.47% removal rate; however, when the duration was increased, the removal rate declined (**Fig. 4d**). Due to more accessible sites in the early stages, it was observed that the metal ion removal rate was rapid, which shows that sorption occurs quickly on the adsorbent's external surface during this phase.

In addition, there was no noticeable variation in the elimination of metal ions after 90 minutes. This is because the adsorbate molecules' solid surface is subject to repulsive forces. As a result, mass transfer between the solid and liquid phases decreases with time. According to [32] equilibrium time is one of the crucial variables for an inexpensive wastewater treatment system.

Effect of agitation speed on As (V) ion adsorption

The agitation of the liquid phase, which influences the mass transfer of metal ions from the bulk liquid to the adsorbent surface, is one of the most significant factors in adsorption processes. To investigate the effects of adsorption, investigations were conducted at five distinct speeds: 40, 60, 80, 100, and 120 rpm. As (V) was initially removed from the aqueous solution with a fast increase; the greatest removal was seen at 60 rpm, and as the agitation speed increased, the removal of As (V) reduced (**Fig. 4c**). Thus, 60 rpm was shown to be the optimal agitation speed.

Conclusion

The effective approach for removing heavy metals from waste water is adsorption by activated carbon. Bio-waste is the most effective, readily available, affordable, and environmentally acceptable adsorbent. Therefore, sugarcane bagasse (ACSB), which is readily available from the sugar industries, was used to prepare activated carbon in the current experiments through physical activation. The observational characteristics revealed that the micropore's volume was significantly larger than the mesoporous material, suggesting that the micropore had a role in the adsorption kinetics. Thus, the activated carbon prepared from sugarcane bagasse (ACSB) may act as good adsorbent due to its high adsorption capacity, high surface area, micropore structure and a high degree of surface. The chemical composition and pore structure of ACSB typically determined the sorption activity of the materials. The surface structure of ACSB showed cleaner tunnels with honey comb like structures. The optimum dose was observed at 2.0 g/100 ml, in which nearly 88% of As (V) ions were removed while optimal pH was 8 at

which nearly 86% of As removed and the optimal agitation speed and time were observed 60 rpm and 90 minutes at which 88.5% and 88.47% As(V) were removed respectively.

Acknowledgement

The author is thankful to the Thematic Unit of Excellence on Soft Nanofabrication and Advanced Imaging Centre, IIT Kanpur and acknowledged for BET analysis, SEM, EDX and XRD images of activated carbon prepared from sugarcane bagasse.

REFERENCES

- [1] Singh, N., Kumar, D., & Sahu, A. P. (2007). *Arsenic in the environment: Effects on human health and possible prevention*. *Journal of Environmental Biology*, 28, 359-365. Retrieved from <https://bit.ly/3gNBL4r>
- [2] Choong, T. S. Y., Chuah, T. G., Robiah, Y., Gregory Koay, F. L., & Azni, I. (2007). *Arsenic toxicity, health hazards and removal techniques from water: An overview*. *Desalination*, 217, 139-166. Retrieved from <https://bit.ly/3fJ38Lw>
- [3] Centeno, J. A., Mullick, F. G., Martinez, L., Page, N. P., & Gibb, H. (2002). *Pathology related to chronic arsenic exposure*. *Environmental Health Perspectives*, 110, 883-886. Retrieved from <https://bit.ly/2XOFMxS>
- [4] Bothe, J. V., & Brown, P. W. (1999). *Arsenic immobilization by calcium arsenate formation*. *Environmental Science & Technology*, 33, 3806-3811. Retrieved from <https://bit.ly/33Mr4Lz>
- [5] Ng, J. C., Wang, J., & Shraim, A. (2003). *A global health problem caused by arsenic from natural sources*. *Chemosphere*, 52, 1353-1359. Retrieved from <https://bit.ly/2PHInW2>
- [6] Singh, R., Singh, S., Parihar, P., Singh, V. P., & Prasad, S. M. (2015). *Arsenic contamination, consequences and remediation techniques: A review*. *Ecotoxicology and Environmental Safety*, 112, 247-270. Retrieved from <https://bit.ly/2DE0TvW>
- [7] Kartinen Jr, E. O., & Martin, C. J. (1995). *An overview of arsenic removal processes*. *Desalination*, 103, 79-88. Retrieved from <https://bit.ly/3krA7HM>
- [8] World Health Organization. (2011). *Guidelines for drinking water quality*. Geneva: WHO, 178. Retrieved from <https://bit.ly/3fLo0li>
- [9] Baskan, M. B., & Pala, A. (2010). *A statistical experiment design approach for arsenic removal by coagulation process using aluminum sulfate*. *Desalination*, 254, 42-48. Retrieved from <https://bit.ly/33N01Or>
- [10] Neppolian, B., Celik, E., & Choi, H. (2008). *Photochemical oxidation of arsenic(III) to arsenic(V) using peroxydisulfate ions as an oxidizing agent*. *Environmental Science & Technology*, 42, 6179-6184. Retrieved from <https://bit.ly/3gNCtP9>
- [11] Katsoyiannis, I. A., Zouboulis, A. I., & Jekel, M. (2004). *Kinetics of bacterial As(III) oxidation and subsequent As(V) removal by sorption onto biogenic manganese oxides during groundwater treatment*. *Industrial & Engineering Chemistry Research*, 43, 486-493. Retrieved from <https://bit.ly/31IAwb>
- [12] Xu, Y., Yang, H., Sun, W., Ge, H., & Yao, R. (2015). *The oxidation of As(III) in groundwater using biological manganese removal filtration columns*. *Environmental Technology*, 36, 2732-2739. Retrieved from <https://bit.ly/31EdpDL>
- [13] Saitua, H., Gil, R., & Padilla, A. P. (2011). *Experimental investigation on arsenic removal with a nanofiltration pilot plant from naturally contaminated groundwater*. *Desalination*, 274, 1-6. Retrieved from <https://bit.ly/30KZqgb>

[14] Zhang, G., Li, X., Wu, S., & Ping, G. (2012). Effect of source water quality on arsenic (V) removal from drinking water by coagulation/microfiltration. *Environmental Earth Sciences*, 66, 1269-1277. Retrieved from <https://bit.ly/3alUdyI>

[15] Baskan, M. B., & Pala, A. (2009). Determination of arsenic removal efficiency by ferric ions using response surface methodology. *Journal of Hazardous Materials*, 166, 796-801. Retrieved from <https://bit.ly/31J8stz>

[16] Wan, W., Pepping, T. J., Banerji, T., Chaudhari, S., & Giammar, D. E. (2011). Effects of water chemistry on arsenic removal from drinking water by electro-coagulation. *Water Research*, 45, 384-392. Retrieved from <https://bit.ly/3kxt0Oa>

[17] Mohan, D., & Pittman, C. U. (2007). Arsenic removal from water/wastewater using adsorbents-A critical review. *Journal of Hazardous Materials*, 142, 1-53. Retrieved from <https://bit.ly/3fJK1kn>

[18] Goswami, A., Raul, P. K., & Purkait, M. K. (2012). Arsenic adsorption using copper (II) oxide nanoparticle. *Chemical Engineering Research and Design*, 90, 1387-1396. Retrieved from <https://bit.ly/3fJJ5wE>

[19] Awual, M. R., Shenashen, M. A., Yaita, T., Shiwaku, H., & Jyo, A. (2012). Efficient arsenic(V) removal from water by ligands exchange fibrous adsorbent. *Water Research*, 46, 5541-5550. Retrieved from <https://bit.ly/2DFMkIp>

[20] Gupta, A., Kumar, V., Singh, P., Verma, L., Pratap, S. G., & Singh, P. K. (2023). Removal of arsenic from contaminated water: Phytoaccumulation and adsorbent-based removal by activated carbon prepared from *Typha tripholia*. *Journal of Environmental Biology*, 44, 594-601.

[21] Kalderis, D., Bethanis, S., Paraskeva, P., & Diadopolos, E. (2008). Production of activated carbon from bagasse and rice husk by a single-stage chemical activation method at low retention times. *Bioresource Technology*, 99(15), 6809-6816.

[22] Xu, Y., He, S., Deng, F., Pang, Q., Xu, Y., & Yao, H. (2019). Efficient removal of elemental mercury by magnetic chlorinated biochars derived from co-pyrolysis of $Fe(NO_3)_3$ -laden wood.

[23] Caturla, F. M., Molina-Sabio, M., & Rodriguez-Reinoso, F. (1991). Preparation of activated carbon by chemical activation with $ZnCl_2$. *Carbon*, 29(7), 999-1007.

[24] Ioannidou, O., & Zabaniotou, A. (2007). Agricultural residues precursors for activated carbon production-a review. *Renewable and Sustainable Energy Reviews*, 11(9), 1966-2005.

[25] Guo, Y., Tan, C., Sun, J., Li, W., Zhang, J., & Zhao, C. (2020). Porous activated carbon derived from waste sugarcane bagasse for CO_2 adsorption. *Chemical Engineering Journal*, 381, 122736.

[26] Kumar, V., Singh, R., Pratap, G. S., Shalini, & Kumar Singh, P. (2023). Optimization of pH during stabilization of hazardous waste basic chrome sulfate sludge for chromium hexavalent. *International Journal of Research and Analytical Reviews*, 10(2), 256-260. Retrieved from <http://www.ijrar.org/IJRAR23B4182.pdf>

[27] Aljeboree, A. M., Alshirifi, A. N., & Alkaim, A. F. (2017). Kinetics and equilibrium study for the adsorption of textile dyes on coconut shell activated carbon. *Arabian Journal of Chemistry*, 10, S3381-S3393.

[28] Arivoli, S., Hema, M., Karuppaiah, M., & Sarvanan, S. (2008). Adsorption of chromium ion by acid activated low cost carbon-kinetic, mechanistic, thermodynamic and equilibrium studies. *Journal of Chemical Sciences*, 5, 820-831.

- [29] *Wang, J. P., Chen, Y. Z., Wang, Y., Yuan, S. J., & Yu, H. Q. (2011). Optimization of the coagulation-flocculation process for pulp mill wastewater treatment using a combination of uniform design and response surface methodology. Water Research, 45, 5633–5640.*
- [30] *Reddad, Z., Gerente, C., Andres, Y., & Cloirec, P. L. (2002). Adsorption of several metal ions onto a low cost biosorbent: Kinetic and equilibrium studies. Environmental Science & Technology, 36, 2067-2073.*
- [31] *Singh, P., & Verma, L. (2017). Removal of Cadmium [Cd (II)] ion by Activated Carbon Prepared from Eichhornia Crassipes Mart (ACECM). SMS, 9(02), 113-118.*
- [32] *Krishnan, K. A., & Anirudhan, T. S. (2002). Uptake of heavy metals in batch systems by sulfurized steam activated carbon prepared from sugarcane bagasse pith. Industrial & Engineering Chemistry Research, 41, 5085–5093.*